

LIGHT OUTPUT AND ENERGY DISSIPATION MECHANISMS IN CRYSTALLOPHOSPHORS ON THE BASE OF Ce³⁺-DOPED SOLID SOLUTIONS OF YAG-LUAG GARNETS

Y. Zorenko, I. Konstankevych

Laboratory of optoelectronic materials, physical department of Lviv National University, 49 Gen. Chuprynka str., 79044, Lviv, Ukraine

INTRODUCTION

Sources of synchrotron radiation allow one to X-ray images of micron and submicron sizes when one uses scintillator screens in the form of single crystalline films (SCF) deposited by means of liquid phase epitaxy (LPE) on the surface of non-luminescent substrates. An example of an X-ray image detector of resolution $R=1.3-1.5 \mu\text{m}$ with the screen based on $\text{Y}_3\text{Al}_5\text{O}_{12}:\text{Ce}$ SCF of thickness $h=5 \mu\text{m}$ has been described by Koch [1]. A further increase of R can be achieved only by reducing the SCF thickness that, in turns, requires screens with the maximum possible absorption coefficient for X-rays $\eta_{\text{abs}} \sim \rho Z_{\text{eff}}^4$, where Z_{eff} is the effective atomic number of SCF, and the conversion efficiency η is not less than 2-5%.

Among the known garnet compounds the largest values of $Z_{\text{eff}}=58.9$ and $\rho=6.67 \text{ g/cm}^3$ are characteristic of $\text{Lu}_3\text{Al}_5\text{O}_{12}:\text{Ce}$ garnet which is an efficient high response scintillator ($\lambda_{\text{max}}=510 \text{ nm}$ and $\tau=46 \text{ ns}$) with $\eta=2.6 \%$ [2]. This paper is dedicated to an analysis of the possibility of producing the X-ray screens based on the $\text{Lu}_3\text{Al}_5\text{O}_{12}:\text{Ce}$ SCF grown by LPE on $\text{Y}_3\text{Al}_5\text{O}_{12}$ substrates at relatively low cost, and to an investigation of the characteristics of their optical, luminescent and scintillation properties.

SCF MANUFACTURE

We have studied the processes of obtaining $\text{Lu}_3\text{Al}_5\text{O}_{12}$ SCF on $\text{Y}_3\text{Al}_5\text{O}_{12}$ substrates with doping of the former with La^{3+} and Sc^{3+} isoelectronic impurities in order to reduce the mismatch between the SCF and substrate lattice parameters $\Delta a \approx 0.093 \text{ \AA}$ (compositions A and B in Table 1, respectively). The La^{3+} ions are located exclusively in dodecahedral (c)-positions of the garnet lattice, whereas the Sc^{3+} ions at concentrations $x < 0.3$ per formula unit in a 2:3 ratio occupy c- and octahedral (a)-positions, respectively [3]. At higher scandium concentrations predominantly Al^{3+} octahedral sites are replaced according to the nearly linear law [4].

The growth of $\text{Lu}_3\text{Al}_5\text{O}_{12}$ films from the melt solution (MS) using a $\text{PbO}:\text{B}_2\text{O}_3$

(10-12:1 mol/mol) fluxing agent and Lu_2O_3 and Al_2O_3 oxides in a 1:4 mol/mol ratio. The substrates were $\text{Y}_3\text{Al}_5\text{O}_{12}$ wafers in (100) or (111) orientations, with a diameter of 15-36 mm and a thickness of ~0.7 mm. After depositing the $\text{Lu}_3\text{Al}_5\text{O}_{12}$ layers on the $\text{Y}_3\text{Al}_5\text{O}_{12}$ substrates, the SCF contain Y impurities as a result of etching the substrates during the initial stage of the epitaxial growth, and the concentration of these ions increases with the number of samples obtained. By this fact, we obtained a series of the $\text{Lu}_3\text{Al}_5\text{O}_{12}$ SCF with $\text{La}_2\text{O}_3/\text{Y}_2\text{O}_3$ ratios equal to 13:1 and 9:1 mol/mol (compositions A1 and A2 in Table 1). For each composition indicated in Table 1 a series of the SCF at various growth temperatures T_g , from the 885-1040°C range was obtained. The growth rate was 0.6-2.4 $\mu\text{m}/\text{min}$ and the velocity of substrate rotation was ~80 rev./min.

Table 1. Composition (in mol. %) in MS for $(\text{LuYLa})_3\text{Al}_5\text{O}_{12}$ SCF (composition A) and $(\text{LuSc})_3(\text{AlSc})_5\text{O}_{12}$ (composition B)

№	Composition A, mol. %					Composition B, mol. %			
	Lu_2O_3	Y_2O_3	La_2O_3	Al_2O_3	CeO_2	Lu_2O_3	Sc_2O_3	Al_2O_3	CeO_2
1	18.42	0.63	8.23	72.72	-	19.02	6.74	74.21	-
2	18.27	0.90	8.17	72.66	-	18.39	9.80	71.81	-
3	17.78	0.88	7.95	70.69	2.70	17.81	9.49	69.50	3.16
4	17.19	0.85	7.68	68.33	5.95	16.95	9.03	66.14	7.85
5	16.63	0.83	7.43	66.14	8.97	15.99	8.52	62.38	13.09
6	16.22	0.80	7.25	64.49	11.24				

X-ray microanalysis of the composition of a number of SCF from series A and B was carried out for estimation of the segregation coefficients of the different ions in the SCF. For example, sample A6 had the composition close to $\text{Lu}_{3.6}\text{Y}_{0.18}\text{La}_{0.035}\text{Ce}_{0.04}\text{Al}_{4.42}\text{O}_{12}$. This points to the possibility of localization of a significant part of the Lu^{3+} ions in Al^{3+} octahedral sites, which is characteristic of $\text{Lu}_3\text{Al}_5\text{O}_{12}$ crystals obtained from MS [5]. Obviously, this is promoted by SCF doped with Ce^{3+} and La^{3+} ions, which have greater ionic radii than Lu^{3+} .

Fig.1 shows the dependencies of the light output η^1 in the SCF the series of $(\text{LaLuY})_3\text{Al}_5\text{O}_{12}:\text{Ce}$ (curve 1) and $(\text{LuSc})_3(\text{AlSc})_5\text{O}_{12}:\text{Ce}$ (curve 2) compositions on the concentration of the CeO_2 impurity in MS as compared to data for $\text{Y}_3\text{Al}_5\text{O}_{12}:\text{Ce}$ [6]. With increase in the activator concentration for composition A, an increase in the light output up to optimum value of ~9

¹ The scintillation parameters of SCF were measured during the excitation by α -particles from ^{239}Pu in an FEU-110 scintillation unit with reference to the standard scintillator of the $\text{Y}_3\text{Al}_5\text{O}_{12}:\text{Ce}$ SCF with of the light output 10700 photon/MeV using ^{137}Cs .

mol.% is observed. The light output approaches an value of 0.85-0.87 of the best samples of $Y_3Al_5O_{12}:Ce$ composition.

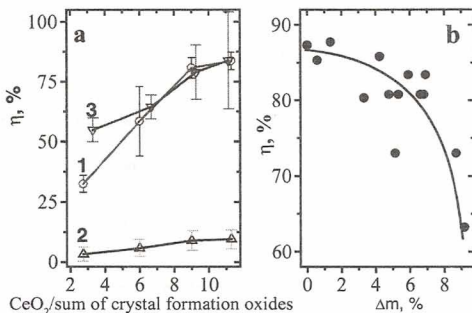


Fig. 1. Dependence of light output in $(LuYLa)_3Al_5O_{12}:Ce$ (1), $(LuSc)_3(AlSc)_5O_{12}:Ce$ (2) and $Y_3Al_5O_{12}$ (3) SCF series on relative concentration of activated impurity $CeO_2/\text{sum of crystal formation oxides}$ in MS (a) and the change in the energy output of the SCF under increasing mass of the obtained samples (change in mass of crystal formation components Δm , %). Number of points on the curve corresponds to N (b)

The differences in the η magnitudes in each SCF series is caused by differences in the ratio of the Ce^{3+} activator and quenching by Pb^{2+} impurities in the given range of T_g .

An extraordinary feature of $(LuSc)_3(AlSc)_5O_{12}:Ce$ (B composition) is the appreciably lower light output, amounting to not greater than 6.5 % of the optimum η in the range of optimum CeO_2 concentration in MS (~9 mol.% for the $Y_3Al_5O_{12}$ SCF (curve 2 in Fig 1)). It should be noted that the analogous effect of Ce^{3+} luminescence quenching has been recently observed when doping $Lu_3Al_5O_{12}:Ce$ [3] and $Y_3Al_5O_{12}:Ce$ [7, 8] by other isoelectronic impurities - Ga^{3+} .

We have studied the dependence of the light output η of the SCF of composition A under increasing sample number N, fabricated from the optimum melt composition (Fig.1 b). As compared to the $\eta(N)$ dependence for $Y_3Al_5O_{12}:Ce^{3+}$ [4], a more marked relationship between η and N takes place for composition A, which shows a narrower homogeneity range in the corresponding MS. When varying the crystal forming components in the 0-0.7% interval ($N=10-12$ samples)² the dispersion of η does not exceed 8% whereas at the concentrations larger than 7% a substantial diminution of the SCF light output occurs.

² The melt total weight was ~1 kg, the substrate area 2.2x2.2 cm², the SCF thickness ~ 10 μm .

This is due to the shift of MS saturation temperature to a region of higher temperatures, which gives rise to a reduction in the Ce^{3+} ion segregation coefficient.

SCF content	Location of absorption maxima, eV			Location of emission maxima, eV			
	Ce^{3+}		Pb^{2+}	Ce^{3+}		Pb^{2+}	
	${}^2F_{7/2} \rightarrow 5d$ (E_a^1, E_a^2)	ΔE_a	${}^1S_0 \rightarrow {}^3P_1$	$5d \rightarrow {}^2F_{7/2,5/2}$ (E_e^1, E_e^2)	ΔE_e	$yB(1,2) \rightarrow {}^1A$	
$Y_3Al_5O_{12}:Ce$	3.62 2.69	0.93	4.71	2.36	2.14	0.22	3.54 2.00
A $(LuYLa)_3Al_5O_{12}:Ce$	3.60 2.75	0.85	4.74	2.435	2.265	0.17	3.73 2.07
B $(LuSc)_3(AlSc)_5O_{12}:Ce$	3.54 2.80	0.74	4.805	2.46	2.29	0.17	3.055 2.17

SCF OPTICAL AND LUMINESCENT PROPERTIES

The optical and luminescent properties of epitaxial structures³ using SCFs with various compositions are shown in Fig. 2 a-b. Absorption is caused by the ${}^1S_0 \rightarrow {}^3P_1$ transitions in the Pb^{2+} ions with $\lambda_{max}=260$ nm [4, 9], whose doping presents the permanent factor in the SCF synthesis from the Pb-containing MS, as well as by the allowed electro-dipole transitions with the E_a^1 and E_a^2 energies from the ${}^2F_{7/2}$ ground state of 4f-shell on the levels of the low doublet of 5d shell of the Ce^{3+} ion [8] (Table 2). Varying the crystal field strength, which is proportional to the magnitude of $\Delta E_a = E_a^1 - E_a^2$, results in a shift of the given bands for compositions A and B with respect to similar bands for $Y_3Al_5O_{12}:Ce^{3+}$ (Table 2).

Table 2. Parameters of absorption and luminescence spectra of $(LuYLa)_3Al_5O_{12}:Ce$ (A content), $(LuSc)_3(AlSc)_5O_{12}:Ce$ (B content) and $Y_3Al_5O_{12}:Ce$ SCF grown from lead-containing MS

³ This term refers to the structure consisting from the $Y_3Al_5O_{12}$ substrate with an SCF on both sides.

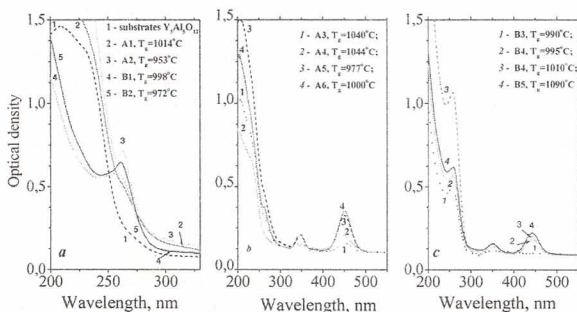


Fig. 2. Absorption spectra of epitaxial structures with: a - nonactivated SCF obtained from MS of compositions: A1 (2), A2 (3) and B1 (4), B2 (5) at different T_g ; b, c - doped with Ce^{3+} SCF obtained from MS of compositions A2-A6 (1-4) and B3-B5 (1-4), respectively. Thickness of SCF $h=10 \mu\text{m}$. In Fig. 2 a, curve 1 - absorption spectrum of $Y_3Al_5O_{12}$ substrate of 0.7 mm thickness is plotted for comparison

A characteristic feature of absorption of the Ce^{3+} -doped SCF is the differences in the absorption dependencies for the $2^1F_{7/2} \rightarrow 5d$ (E_a^1 , E_a^2) and $1^1S_0 \rightarrow 3^1P_1$ transitions on the growth temperature T_g , corresponding to the different values of $\text{Ce}^{3+}/\text{Pb}^{2+}$ ion concentration ratio. (see, for example, curve 2 and 3 in Fig. 2b.) The optimum is the maximum value of this ratio in the range of the CeO_2 concentration in MS of ~ 9 mol.%, which corresponds to the maximum magnitude of the light output of compositions A and B.

The cathodoluminescent (CL) spectra of the SCF of compositions A and B are plotted in Fig. 3 and Fig. 4 respectively. As seen in Fig. 3a, the emission spectrum of the $\text{Lu}_3\text{Al}_5\text{O}_{12}$ SCF doped by La^{3+} and Y^{3+} (curves 1-2) in the UV spectral region consists of the superposition of two bands with $\lambda_{\text{max}}=267 \text{ nm}$ (4.63 eV) and 284 nm (4.37 eV). With increasing Y concentration the intensity decreases without marked change in the relation between the intensities of the individual bands (curve 3). The above-mentioned features of luminescence of the SCF of composition A may be explained by supposing the formation by La^{3+} and Lu^{3+} isoelectronic impurities in the sites of the Lu^{3+} and Al^{3+} ions, respectively. These are centers of radiative recombination with bands having $h\nu_{\text{max}}=4.63$ and 4.67 eV. The $\text{La}^{3+}_{\text{Lu}}$ ion similarly to $\text{La}^{3+}_{\text{Y}}$ in $Y_3Al_5O_{12}:\text{La}$ [10], forms a split deep level. The latter is a localization center for electrons and formed due large difference in non-Coulomb potential of the isoelectronic impurities which is proportional to the difference of the ionic radii $\Delta=R_{\text{La}}-R_{\text{Lu}}=+0.195 \text{ \AA}$. Recombination of

the localized electrons with the free holes is the cause of luminescence in the band with $h\nu_{\max}=4.63$ eV.

The anti-site $\text{Lu}^{3+}_{\text{Al}}$ defect (Lu in the octa-sites of Al^{3+}), which is inherent to the structure of garnets obtained from MS, represents the analogy to the isoelectronic impurities and forms split level for localization ($\Delta=R_{\text{Al}}-R_{\text{Lu}}=-0.33$ Å [10]) of holes whose recombination with free electrons is accompanied with luminescence in the 4.67 eV band. In the meantime, the concentration of such centers in SCF on the basis of $\text{Lu}_3\text{Al}_5\text{O}_{12}$ obtained from MS should be minimal [10, 11]. The intensity of the 4.37 eV band which is comparable with the $\text{La}^{3+}_{\text{Lu}}$ center emission can be explained only by significant increase of the $\text{Lu}^{3+}_{\text{Al}}$ center concentration because of the known "replacement" effect of ions with smaller ionic radius (Lu^{3+}) in *a*-sites of garnet lattice [5] by ions with larger ionic radius (La^{3+}) what takes place due to the fact that Y^{3+} ions during substitution by Lu^{3+} do not form split out levels as a result of small magnitude of $R_{\text{Lu}}-R_{\text{Y}}=-0.04$ Å [10].

The CL spectrum of the SCF (composition B) represents the superposition of the two bands with $\lambda_{\max}=290$ nm (4.26 eV) and 324 nm (3.82 eV) (fig. 4a, curves 1-3), with the ratio of their intensities being a function of the Sc concentration. For composition of Sc_2O_3 in MS equal to 7 mol.% (composition B1) the dominant is the 4.26 eV band, whereas at increasing the Sc_2O_3 concentration to 10 mol.% the main luminescence maximum shifts in the long wave-length range at the expense of more intensive 3.83 eV component (Fig. 4a, insert). The above mentioned behavior of the emission spectra in the SCF of composition B under growing the Sc concentration is consistent mainly with the data for the $\text{Y}_3\text{Al}_5\text{O}_{12}:\text{Sc}$ SCF [12] what enables to interpret the bands with $h\nu_{\max}=4.26$ and 3.82 eV as a recombination luminescence of the $\text{Sc}^{3+}_{\text{Lu}}$ and $\text{Sc}^{3+}_{\text{Al}}$ centers under substitution by Sc the ground Lu^{3+} and Al^{3+} ions respectively in the dodecahedral and octahedral positions of the garnet lattice.

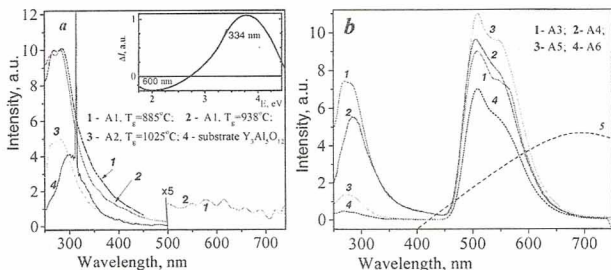


Fig. 3. CL spectra of $(LuYLa)_3Al_5O_{12}$ SCF (compositions A1, A2) (a) and $(LuYLa)_3Al_5O_{12}:Ce$ (compositions A3-A6) (b). Spectrum of $Y_3Al_5O_{12}$ substrate (a, curve 4) and dependence of spectral sensitivity of CCD array of X-ray detector [1] (b, curve 5) are given for comparison. Insert - difference spectrum of SCF of A1 composition obtained at $T_g = 885^\circ C$ (1) and $938^\circ C$ (2) which corresponds to Pb^{2+} ions emission

Analysis of the differences in emission spectra of the SCF of A and B composition manufactured at various T_g , that corresponds to the different degree of the Pb impurities, allows to extract (Fig. 3 a and Fig. 4 a, inserts) the characteristic for the emission of mercury like Pb^{2+} ions in garnets [4, 9] the doublet structure of the emission bands, as well as the location of their maxima (Table 2). In the CL spectra of the SCF of composition A and B (Fig. 3b and Fig. 4b) one can see the doublet emission band in the 450-700 nm connected with the allowed $5d \rightarrow 4f^2(F_{5/2,7/2})$ transitions of the Ce^{3+} ions. Increase in the crystal field strength proportional to the difference of these transitions energy $\Delta E = E_e^1(F_{5/2}) - E_e^2(F_{7/2})$ for the garnets of compositions A and B in comparison with $Y_3Al_5O_{12}:Ce$ leads to the shift of Ce^{3+} emission bands in the short wave length range (Table 2) and change in the SCF emission color.

Under increasing the activator concentration the relative contribution of the Ce^{3+} ions emission in the SCF light output goes up under corresponding reduction of UV luminescence intensity of the centers formed by isoelectronic impurities (Fig. 3 b and Fig. 4 b). This to large extent is characteristic to the SCF of composition A for which in region of the optimum CeO_2 concentration (>9 mol.%) the luminescence is practically quenched. For the SCF of composition B at the optimum CeO_2 concentration the intensity of the emission bands in the visible and UV regions are comparable that shows a strong competition between the Sc_{Lu}^{3+} , Sc_{Al}^{3+} and Ce^{3+} ions at intercepting the excitation energy and, obviously, is one of the causes of the low light output of luminescence.

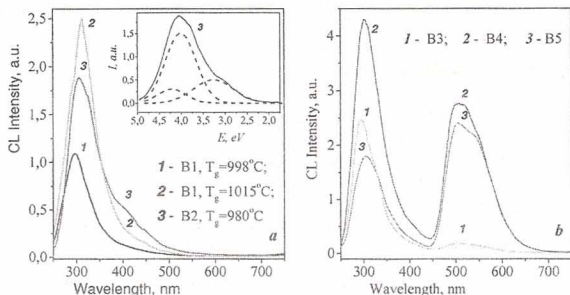


Fig. 4. CL spectra of $(\text{LuSc})_3(\text{AlSc})_5\text{O}_{12}$ (B1 and B2 contents) (a) and $(\text{LuSc})_3(\text{AlSc})_5\text{O}_{12}:\text{Ce}$ (B3-B5 contents) (b)

Meanwhile, in our opinion, the main cause for the significant decrease of the $(\text{LuSc})_3(\text{AlSc})_5\text{O}_{12}:\text{Ce}$ SCF light output is the presence for this compound the effective channel of energy dissipation which is connected with the transitions between the allowed band extrema and activator levels.

Such a mechanism of quenching of luminescence of rare-earth ions with $4f-5d$ transitions we have earlier considered in of $\text{Y}_3\text{Al}_{5-x}\text{Ga}_x\text{O}_{12}:\text{Ce};\text{Pr}$ [12, 13]. Apparently, as in the case of substitution by Ga, the consequence of large (~ 1.3 f. u.) degree of the SCF of composition B by Sc ions lies in the narrowing of the garnet energy gap what results in increase of probability of non-radiative transition between Ce^{3+} ion levels and band structure levels.

CONCLUSIONS

The emission spectrum of the $(\text{LuLaY})_3\text{Al}_5\text{O}_{12}:\text{Ce}$ (Fig. 3b) to large extent overlays with the region of spectral sensitivity of Charge Coupled Devices (CCD) cameras used as radiation detectors [1] (Fig.3, curve 5). The light output of the SCF of this composition under registering the radiation by photodiode with spectral sensitivity close to sensitivity region of frontside illuminated CCD [1] exceeds the $\text{Y}_3\text{Al}_5\text{O}_{12}:\text{Ce}^{3+}$ SCF light output by factor of 1.35-1.4. Estimation of the conversion efficiency value $\sim 7\%$, $\rho = 6.6 \text{ g/cm}^3$ and $Z_{\text{eff}} = 58$, we have obtained for the SCF of this composition in the range of CeO optimum concentration, shows that the increase of X-ray absorption coefficient for screens made on the basis of these SCF is of ~ 7 and 2.5 factors for the 5-17 and 18-60 keV energies, respectively. This allows, according to calculation by the procedure described by Koch [1], to reach at the SCF thicknesses ~ 1.0 -

2.0 μm and aperture of optical system ~ 1.0 the resolution capability of X-ray detector not less than 0.75-1.0 μm .

REFERENCES

- Koch A., Raven C., Spane P. and Snigirev A. X-ray imaging with submicrometer resolution employing transparent luminescent screens. *J. Opt. Soc. Am. A.*, 15 (1998) 1940-1951.
- van Eijk C.W.E., Andriessen J., Dorenbos P., Visser P. Ce^{3+} doped inorganic scintillators. *Nucl. Instr. Meth. A*348 (1994). 546-550.
- Robertson J.M. and van Tol M.V. Cathodoluminescent garnet layers. *Thin Solid Films*, 1-2 (1984). 221-240.
- Zorenko Yu.V., Batenchuk M.M., Gorbenko V.I., Konstankevych I.V. Factors, depending on energy yield of luminophores on the base single crystalline $\text{Al}_2\text{O}_3\text{-Y}_2\text{O}_3$ R_2O_3 oxides. *Zhurnal Prikladnoi Spektroskopii*, 67 (1999). 241-246.
- Ashurov M.Kh., Voron'ko Yu.K., Osiko V.V., Sobol' A.A. The spectroscopic investigation of structure disorder of garnet crystals with rare earth elements. In *Spectroscopy of Crystals*, Nauka, Moscow, (1978). 71-83.
- Zorenko Yu.V., Malutenkov P.S., Patsagan N.I., Nazar I.V., Gorbenko V.I., Batenchuk M.M., Pashkovsky M.V. The peculiarities of receiving of thin films of single crystals oxide luminophors. *Crystal Properties and Preparation*, 36-38 (1991). 223-226.
- Robertson J.M., van Tol M.V. and Smith G. Colourshift of the Ce^{3+} -emission in monocrystalline epitaxial grown garnet layers. *Philips Journal of Research*, 36 (1981). 15-29.
- Zorenko Yu.V., Nazar I.V., Lymarenko L.N., Pashkovsky M.V. The luminescence of Ce^{3+} ions in solid solution $\text{Y}_3\text{Al}_5\text{O}_{12}\text{-Y}_3\text{Ga}_5\text{O}_{12}$. *Optika i Spektroskopia*, 80 (1996). 925-928.
- Scott G.B., and Page J.L. Pb-valence in garnets. *J. Appl. Phys.*, 48 (1977). 1342-1349.
- Zorenko Yu.V. Isoelectronic impurities as luminescence centers in the oxide with garnet structure. *Optika i Spektroskopia*, 84 (1998). 856-860.
- Zorenko Yu.V., Pashkovsky M.V., Batenchuk M.M., Limarenko L.N., Nazar I.V. Antisite defects in luminescence of crystallophosphors with garnet structure. *Optics and Spectroscopy*, 80 (1996). 776-780.
- Valbis Y., Volzhenska L.G., Dubov Yu.G., Zorenko Yu.V., Nazar I.V., Patsagan N.I., Pashkovsky M.V. The luminescent centers in single crystalline compounds of yttrium-aluminium garnets, doped by scandium isoelectronic impurities. *Optika i Spektroskopia*, 63 (1987). 1058-1064.
- Zorenko Yu.V., Limarenko L.N., Nazar I.V., Pashkovsky M.V. The luminescence of Pr^{3+} ions in solid solution $\text{Y}_3\text{Al}_{5-x}\text{Ga}_x\text{O}_{12}\text{:Pr}$. *Zhurnal Prikladnoj Spektroskopii*, 55 (1991). 774-778.